

# EVALUAREA PERFORMANTELOR STÂLPILOR DIN BETON CONSOLIDAȚI CU MATRICE PE BAZĂ DE CIMENT ARMATĂ CU FIBRE (FRCM) PERFORMANCE EVALUATION OF CONCRETE COLUMNS STRENGTHENED WITH FIBRE REINFORCED CEMENTITIOUS MATRIX (FRCM)

HUSSEIN HAKIM HASAN\*, RADU PASCU, DAN PAUL GEORGESCU

Civil Department, Technical University of Civil Engineering of Bucharest, 122-124 Lacul Tei Bvd., Bucharest, Romania

*The Fibre Reinforced Cementitious Matrix (FRCM) composite material is a relatively new retrofitting system which is used to increase the strength and overall ductility of concrete structures. This paper presents a comparative study on the performance of concrete columns confined with FRCM, using the experimental, finite element method (FEM) and analytical evaluation techniques. Six concrete columns were experimentally tested under monotonic uniaxial compression loading: two specimens without confinement, two specimens with one FRCM layer and two specimens with two FRCM layers. Material tests were also performed on concrete cubes, for each concrete column. A complex nonlinear numerical FEM tridimensional model was developed in Abaqus finite element environment for each concrete column and calibrated against the experimental results. Calibration for each concrete material was also performed, assuming the Eurocode 2 model for obtaining the stress-strain curves used to characterize the behavior of concrete under uniaxial compression. Concrete Damaged Plasticity Model (CDPM) was assigned to the concrete parts. The performance of columns is evaluated in terms of axial load carrying capacity, axial compressive strength, ultimate axial deformation and strain. FEM results also revealed the cross-section distribution of the confining stresses due to FRCM. Analytical predictions according to several researchers are also presented in view of comparison.*

*Sistemul cu plase de armare din fibre de carbon inglobate într-o matrice de mortar bicomponent pe bază de ciment (FRCM) reprezintă o metodă relativ nouă de consolidare care este utilizat în scopul îmbunătățirii rezistenței și ductilității structurilor din beton. Articolul prezintă un studiu comparativ al performanțelor unor stâlpi confinați cu FRCM rezultate atât prin efectuarea unor cercetări experimentale cât și prin aplicarea unor relații de calcul analitice și a metodei elementelor finite (FEM). S-au încercat 6 stâlpi, 2 stâlpi de referință neconsolidați, 2 stâlpi la care s-a aplicat un strat de FRCM și 2 stâlpi la care s-au aplicat 2 straturi de FRCM. Pentru analiza comportării stâlpilor s-a dezvoltat un model neliniar tridimensional FEM cu ajutorul programului Abaqus pentru fiecare din stâlpii încercați experimental. De asemenea comportarea stâlpilor sub solicitări a fost analizată în conformitate cu Eurocode 2 în scopul obținerii curbelor efort unitar - deformație specifică ale stâlpilor supuși la compresiune axială. Modelul de beton cu plasticitate deteriorată a fost atribuit componentelor din beton. Performanțele stâlpilor au fost evaluate în termeni de forța ultimă la compresiune și în deformații axiale și deformații specifice. Datele obținute experimental au fost comparate de asemenea cu cele rezultate prin aplicarea unor relații de calcul propuse de diverși cercetători.*

**Keywords:** plain concrete column, FRCM, confinement, FEM, CDPM, analytical model

## 1. Introduction

Reinforced concrete structures are subjected to degradation due to many causes, including loads beyond the design one, design and construction errors, exposure to the environmental conditions, moisture and others. Throughout the years, researchers have proposed many retrofitting techniques (steel / concrete / fiber mesh jacketing) to strengthen or repair the degraded structures. One of the common retrofitting techniques of concrete columns is to apply a fibre mesh all-around of the cross-section by using a bonding agent (adhesive, mortar), thus creating a confining jacket. This technique increases both the axial capacity and the ductility of the column. Other advantages are the high strength-to-weight ratio, corrosion resistance and speed of application. Fibre jacketing has disadvantages related to the organic matrices, which are combustible and requires special treatment of

the surface of the retrofitted element prior its application. Fibre Reinforced Cementitious Matrix FRCM material was proposed as a retrofitting system to overcome the limitations related with the use of organic adhesives. FRCM system consists of high strength fibre mesh and cementitious mortar. FRCM has several advantages over the traditional fibre jacketing: it is less affected by temperature fluctuations, it is inherently incombustible, possesses porous properties, can be applied to concrete elements in low temperature conditions and on wet surfaces, is an effective retrofit system for concrete elements loaded in compression [1-6].

Since the FRCM is a relatively recent strengthening system, therefore, the number of experimental [1-3] and numerical [7] research on FRCM confined concrete columns is limited. Different parameters were investigated (cross-section shape, eccentricity, ratio and orientations of fibres) and the outcome of the studies was that the

\* Autor corespondent/Corresponding author,  
E-mail: [hossainhakem@yahoo.com](mailto:hossainhakem@yahoo.com)

FRCM increased the strength and the ductility of specimens. The objective of this paper is to present a comparative study on the performance of concrete columns confined with different number of layers of FRCM, using the experimental, finite element method FEM and analytical evaluation techniques.

## 2. Summary of experimental tests

The experimental program (Table 1) consisted of six monotonic uniaxial compression tests on short plain concrete columns of square cross-section (Figure 1), being strengthened with various number of FRCM layers. Two specimens CP-1 and CP-2 were not confined with FRCM as to be considered as reference, while for the other specimens the number of layers of FRCM, cross-sectional area and compressive strength of concrete material varied. The variation of the cross-section for the other specimens is due to the FRCM system. The thickness of the FRCM jacket depends on the number of layers of fibre mesh, because a 0.5 cm layer of mortar is required before and after application of a layer of mesh.

A low-strength C16/20 concrete material was used for the columns. Cube samples (15x15x15 cm) were taken from each cast and tested under uniaxial compression 28 days after curing [8, 9], and their average compressive strengths are summarized in Table 1. A high-strength carbon fibre with 1x1 cm mesh, Mapegrid C170 [10], was used to confine the columns, with a tensile strength of 5000 N/mm<sup>2</sup>. The modulus of elasticity is 252000 N/mm<sup>2</sup>, while the elongation at failure is 2%. The equivalent thickness of the dry fabric is 0.048 mm. Planitop HDM [11] mortar was used as matrix for FRCM system. According to data sheet, the compressive strength after 28 days reaches at least 28 N/mm<sup>2</sup>, while the compressive modulus of elasticity is 11000 N/mm<sup>2</sup>.

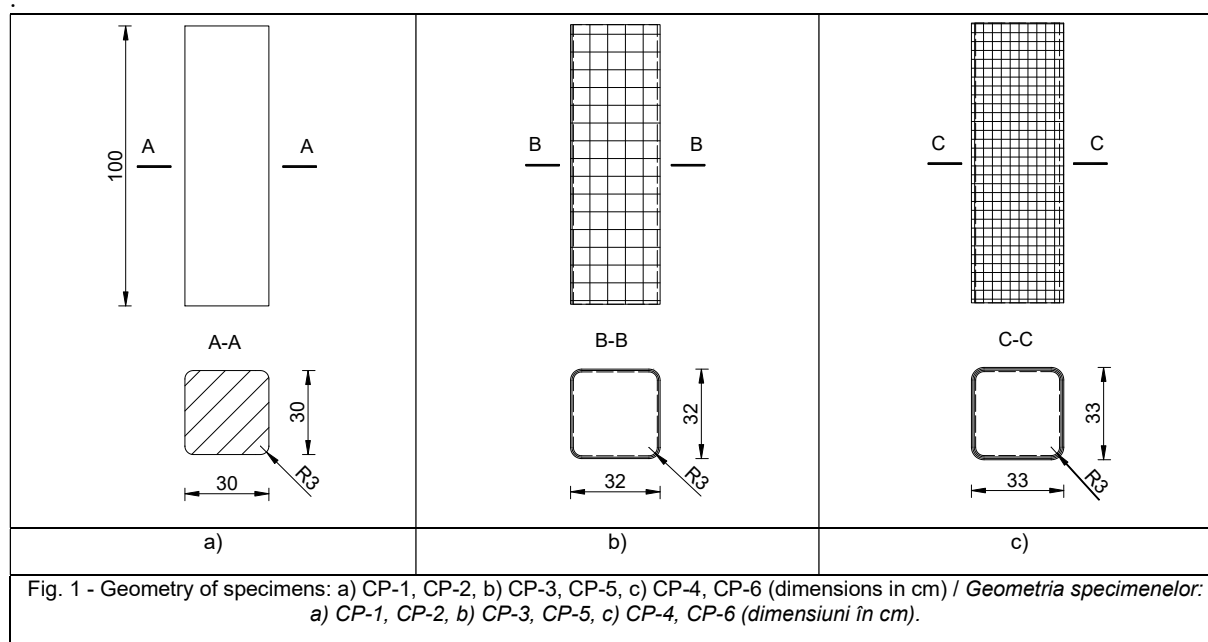
The experimental setup for the columns aimed to assure uniaxial centric compression by placing the columns vertically and centered to the steel plates. The reaction force recorded by the testing machine and the axial deformation measured using mechanical dial gauge were monitored. The axial stress was obtained by dividing the reaction force to the initial cross-sectional area of the column. The axial strain was

Table 1

The experimental program / Programul experimental

Specimen	Cross-section area (cm)	$f_{c,cube}$ (N/mm <sup>2</sup> )	No. of FRCM layers
CP-1	30x30	22.50	-
CP-2	30x30	24.54	-
CP-3	32x32	21.00	1
CP-4	33x33	21.00	2
CP-5	32x32	20.00	1
CP-6	33x33	20.00	2

\*  $f_{c,cube}$  is the compressive strength of plain concrete determined from cube samples.



Specimen	FRCM layers	$N_{max}$ (kN)	$N_{max,ave}$ (kN)	$N_{max}$ increase (%)	$f_{c,exp} = N_{max}/A_c$ (N/mm <sup>2</sup> )	$f_{c,cube}$ (N/mm <sup>2</sup> )	$f_{c,initial}^{***}$ (N/mm <sup>2</sup> )	$f_{c,exp}/f_{c,initial}^{***}$ (-)	$f_{c,exp}/f_{c,initial}^{***}$ average increase (%)	$D$ (mm)	$\epsilon_{max}$ (mm/mm)
CP-1	-	1830	1875	-	20.33	22.50	20.25	1.00	-	0.505*	0.001009*
CP-2	-	1920			21.33	24.54	22.1	0.965		0.445*	0.000889*
CP-3	1	2130	2122	13.17	23.67	21.00	19.00	1.246	28	0.424*; 0.615**	0.000848*; 0.001230**
CP-5	1	2114			23.49	20.00	18.00	1.305		0.472*; 0.645**	0.000944*; 0.001289**
CP-4	2	2160	2147.5	14.53	24.00	21.00	19.00	1.263	29	0.416*; 0.567**	0.000831*; 0.001133**
CP-6	2	2135			23.72	20.00	18.00	1.318		0.431*; 0.533**	0.000862*; 0.001066**

\* measured at 1500 kN. \*\* measured at 1700 kN. \*\*\*  $f_{c,initial} = (f_{c,ave,exp} CP-1;2 / f_{c,ave,cube} CP-1;2) \times f_{c,cube} CP-3;4;5;6$ .  $A_c$  cross-sectional

obtained by dividing the monitored deformation to the initial gauge length of 50 cm.

The column performance is evaluated through the parameters axial load carrying capacity  $N_{max}$ , axial compressive strength  $f_{c,exp}$ , maximum axial deformation  $D$ , maximum axial strain  $\epsilon_{max}$ . The results are grouped based on the number of FRCM layers provided (reference, 1, 2 layers) and summarized in Table 2.

Adding one layer of FRCM provided the specimens CP-3 and CP-5 with an additional 13.17% capacity, relative to average capacity of reference specimens CP-1 and CP-2. A 14.53% capacity increase was obtained for two-layer specimens CP-4 and CP-6, relative to the reference average capacity. The axial compressive strength obtained from the columns is compared with the initial compressive strength  $f_{c,initial}$  which is about 0.9 of the compressive strength of the cube. The increment in compressive strength was with an average ratio of 28% for one FRCM layer specimens and 29% for two FRCM layer specimens. Thus, there is a small difference in compressive strength between one and two FRCM layers specimens. Similar results are presented in the literature [12, 13] where the cementitious mortar was used as the matrix.

Due to the damage of the exterior surface of columns caused by cracking during testing, the measurements of the axial deformation  $D$  were possible up to 1500 kN for CP-1 and CP-2 and up to 1700 kN for the other specimens. Table 2 presents the values at both force level, where available, in view of comparison. It can be observed that the use of FRCM system reduced the maximum deformation for the same level of axial force; for example, in case of unconfined specimen CP-1 the deformation at 1500kN is 0.505 mm, while for one-layer FRCM specimen CP-3 the corresponding deformation is 0.424 mm. Also, using two layers of FRCM (CP-4, CP-6) slightly reduces the deformation with respect to one-layer specimens

(CP-3, CP-5); for example, in case of one-layer specimen CP-3 the deformation at 1500kN is 0.424 mm, while for two-layer FRCM specimen CP-4 the corresponding deformation is 0.416 mm. The maximum strains summarized in Table 2 follow the same trend as the deformation.

In Figure 2 are presented the experimental axial force-deformation curves (CP-1 to CP-6), the maximum recorded force  $F_{max}$  for all specimens in comparison with the results from the finite element method FEM.

The failure mode of the specimens was also monitored. In the case of specimens confined by FRCM jackets the failure was observed at/near mid-height of the specimens. The failure starts as a crack at mid-height of specimen and starts to vertically grow to extremities of the specimen until the failure occurs (Figure 4). As the axial load increased, the cracks continued to grow in length and width, which indicated slippage of the fibres, and the concrete started to crush inside the carbon FRCM jacket. While increasing the axial load, the cracks initiate at about 95 % of the maximum axial load applied, then the failure occurred suddenly. Full detachment of the carbon FRCM jackets was not observed, but for some specimens, small parts of the mortar layer were easily removed after the specimens were unloaded. The failure mode of confined specimens was less brittle than that observed for unconfined specimens.

### 3. Finite element analysis

#### 3.1. Material models

Using the provisions from Eurocode 2-1-2004 [8] the mechanical properties of concrete material were determined and summarized in Table 3. The behavior of concrete material was modeled using isotropic linear elasticity and nonlinear plasticity. The elastic behavior is defined by the reduced elastic modulus  $E_c$ , which varies among the concrete materials, and the Poisson's ratio

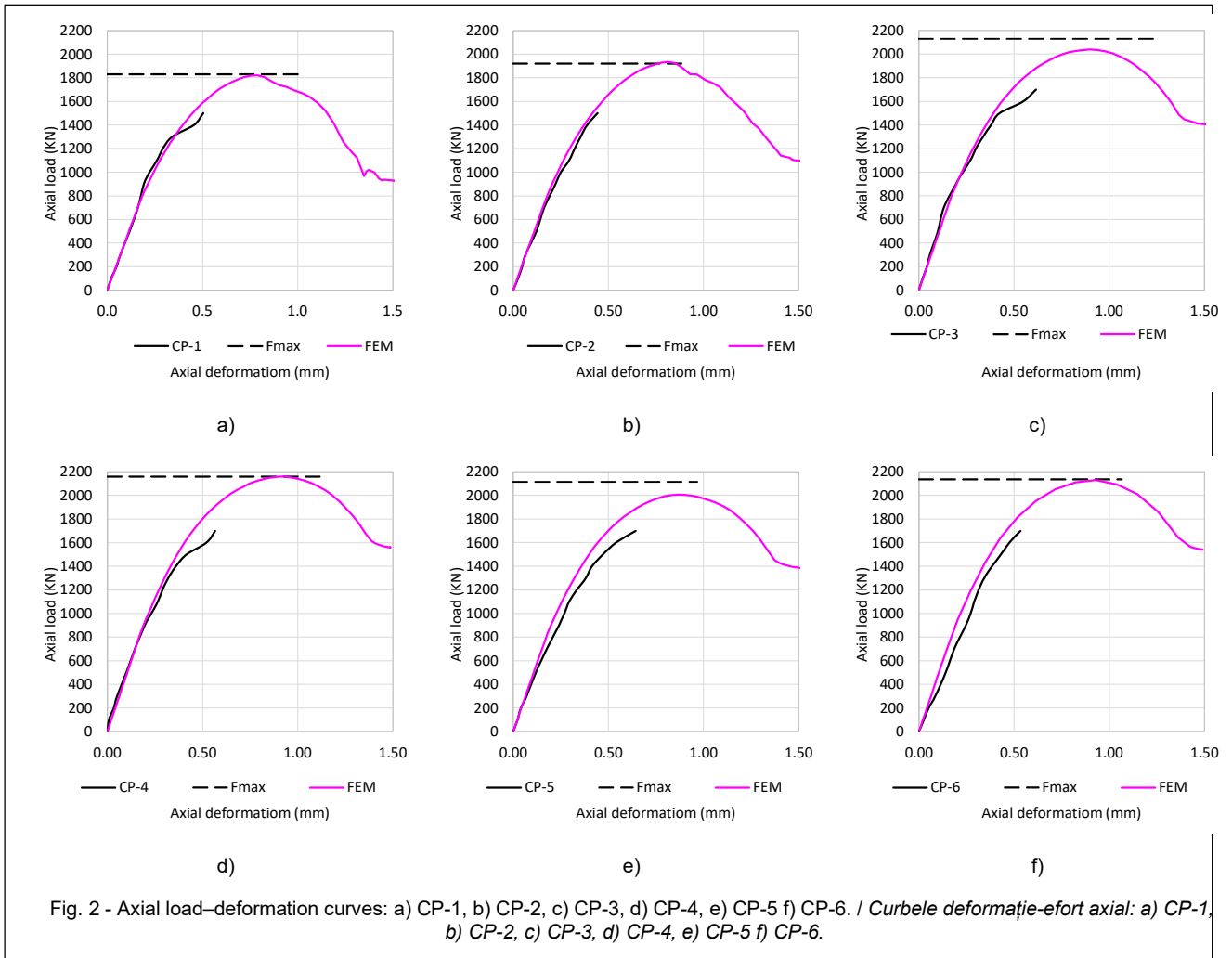


Fig. 2 - Axial load–deformation curves: a) CP-1, b) CP-2, c) CP-3, d) CP-4, e) CP-5 f) CP-6. / Curbele deformație-efort axial: a) CP-1, b) CP-2, c) CP-3, d) CP-4, e) CP-5 f) CP-6.

Mechanical properties of concrete / Proprietățile mecanice ale betonului								
ID	$f_{cm,cube}$ (N/mm <sup>2</sup> )	$f_{cm}$ (N/mm <sup>2</sup> )	$0.4f_{cm}$ (N/mm <sup>2</sup> )	$f_{ck}$ (N/mm <sup>2</sup> )	$f_{ctm}$ (N/mm <sup>2</sup> )	$E_{cm}$ (N/mm <sup>2</sup> )	$e_{c1}$ (mm/mm)	k
CP-1	22.50	21.56	8.70	13.56	1.71	27701	0.00181	2.45
CP-2	24.54	22.76	9.11	14.76	1.81	28157	0.00184	2.40
CP-3, CP-4	21.88*	21.18	8.50	13.18	1.67	27556	0.00180	2.46
CP-5, CP-6	21.35**	20.87	8.40	12.87	1.65	27431	0.00179	2.48

- $f_{cm,cube}$ , mean value of concrete cube compressive strength, experimentally determined at 28 days.
- $f_{ck,cube} = (1 - 1.64 \cdot c_v) \cdot f_{cm,cube}$ , characteristic compressive cube strength of concrete.
- $c_v = s/f_{cm,cube}$ , coefficient of variation of the standard deviation ( $c_v = 0.15$ , according to [15]).
- $s$ , standard deviation.
- $f_{ck} = 0.8 \cdot f_{ck,cube}$ , characteristic compressive cylinder strength of concrete.
- $f_{cm} = f_{ck} + 8$  N/mm<sup>2</sup>, mean value of concrete cylinder compressive strength.
- $0.4 \cdot f_{cm}$ , linear elastic compressive limit.
- $f_{ctm} = 0.3f_{ck}^{2/3}$ , mean value of axial tensile strength of concrete.
- $E_{cm} = 22 \cdot [(f_{cm})/10]^{0.3}$ , ( $f_{cm}$  in N/mm<sup>2</sup>) secant modulus of elasticity of concrete.
- $E_c = (0.4 \cdot f_{cm}) / e_{c0.4f_{cm}}$ , ( $f_{cm}$  in N/mm<sup>2</sup>) reduced modulus of elasticity of concrete.
- $e_{c1} = 0.7 \cdot f_{cm}^{0.31}$ , compressive strain in the concrete at the peak stress  $f_{cm}$ .
- $k = 1.05 \cdot E_{cm} \cdot |e_{c1}| / f_{cm}$ , plasticity number.

Notes:  
 \* 0.88 N/mm<sup>2</sup> was added to the experimental value 21 N/mm<sup>2</sup> as to obtain closer fitting on tested columns F-D response.  
 \*\* 1.35 N/mm<sup>2</sup> was added to the experimental value 20 N/mm<sup>2</sup> as to obtain closer fitting on teste columns F-D response.

which was set 0.2. The modelling approach of the plastic behavior is using the Abaqus built-in Concrete Damaged Plasticity Model, CDPM [14]. The definition of the plasticity is according to [14]:

dilation angle = 31°; eccentricity = 0.1; ratio of initial equibiaxial compressive yield stress to initial uniaxial compressive yield stress  $f_{bol}/f_{c0} = 1.16$ ; ratio of the second stress invariant on the tensile

Table 4

Mechanical properties of FRCM / <i>Proprietățile mecanice ale FRCM</i>							
Elastic type	Material property						
Lamina	$E_1$ [N/mm <sup>2</sup> ]	$E_2$ [N/mm <sup>2</sup> ]	$\nu_{12}$ [-]	$G_{12}$ [N/mm <sup>2</sup> ]	$G_{13}$ [N/mm <sup>2</sup> ]	$G_{23}$ [N/mm <sup>2</sup> ]	
	252000	252000	0.1	0.1	0.1	0.1	
Sub-option	Material property						
Fail stress	$X_t$ [N/mm <sup>2</sup> ]	$X_c$ [N/mm <sup>2</sup> ]	$Y_t$ [N/mm <sup>2</sup> ]	$Y_c$ [N/mm <sup>2</sup> ]	$S$ [N/mm <sup>2</sup> ]	* $f$ [-]	$s_{biax}$ [N/mm <sup>2</sup> ]
	5000	0.1	5000	0.1	0.1	0	5000

meridian to that on the compressive meridian  $K = 0.667$ ; viscosity parameter = 0. The linear elastic compression limit was considered equal to  $0.4f_{cm}$ , and the definition of the compressive nonlinear behavior of concrete material was based on Eurocode 2-1-1/2004 [8] provisions for nonlinear analyses. The engineering compressive stress-strain curve ( $s$ - $e$ ) was then transformed into true stress-strain curve ( $\sigma$ - $\varepsilon$ ). The true value of reduced modulus of elasticity of concrete  $E_{c,true}$  was determined from the true stress-strain curve and used within simulations. The input for compressive behavior in Abaqus is the plastic stress  $\sigma_{c,pl,i}$  and the inelastic strain  $\varepsilon_{c,in,i}$ . The first value of  $\varepsilon_{c,pl,0}$  was set the true value of  $0.4f_{cm}$ . The inelastic strain  $\varepsilon_{c,in,i}$  was obtained by subtracting the elastic true strain from the total true strain with the formula:  $\varepsilon_{c,in,i} = \varepsilon_{c,i} - \sigma_{c,i}/E_{c,true}$ . A simplified model was adopted for the tensile behavior with the elastic limit of  $f_{ctm}$ , and a negative slope as to consider material degradation.

The FRCM was modeled using the lamina option from Abaqus, which is used to specify orthotropic elastic properties in plane stress. The definition of lamina requires five constants: the Young's moduli in the principal directions  $E_1$  and  $E_2$ , the shear moduli  $G_{12}$ ,  $G_{13}$  and  $G_{23}$ , and the Poisson's ratio  $\nu_{12}$ . Other constants are calculated by the program. To define the plane stress orthotropic failure measures for the material the stress-based failure measures option was used from the sub-options. It requires the definition of the seven strength values: tensile stress limit in the fibre direction  $X_t$ , compressive stress limit in the fibre direction  $X_c$ , tensile stress limit in the transverse direction  $Y_t$ , compressive stress limit in the transverse direction  $Y_c$ , shear strength in the X-Y plane  $S$ , cross product term coefficient  $*f$ , biaxial stress limit  $\sigma_{biax}$ . Since only the uniaxial properties of the FRCM (Mapegrid C 170 [10]) were available in the datasheet, small values were assigned to the unknown parameters as summarized in Table 4 and based on [16].

The mortar was similarly modeled as the concrete by using the isotropic elasticity and CDPM models. The same procedure was used to generate the material input. A maximum compression stress of  $31.8 \text{ N/mm}^2$  was considered for the definition of the input plastic strain – inelastic stress curve. This  $31.8 \text{ N/mm}^2$  value is greater than the valued in the datasheet ( $28 \text{ N/mm}^2$ ) and is based on [5]. The elastic behavior was defined by the reduced elastic

modulus  $E_c$ , which was set equal to  $11000 \text{ N/mm}^2$ , and the Poisson's ratio which was set equal to 0.2. The elastic limit in tension was set equal to  $2 \text{ N/mm}^2$ , and a linear material degradation was considered for the plastic behavior.

The steel plates of the testing machine were modeled using only elastic properties of structural steel: the Young's modulus  $E_s = 210000 \text{ N/mm}^2$  and the Poisson's ratio 0.3.

### 3.2. Column models

Finite element models were created for each column specimen. All column models have several common features: types of finite elements, material models, boundary conditions, contact laws. The differences between the models relate to geometry and material input (see Figure 3 a) and b)).

The concrete and mortar parts were modelled using eight-node linear elements (C3D8R), with a global mesh size of 10 mm. The FRCM was modeled using 4-node quadrilateral membrane finite elements (M3D4R), with a mesh size of 10 mm. The steel plates were modeled with C3D8R with a mesh size of 20 mm.

As regarding the constraints, two reference points (RP1, RP2) were created at the extremity of the column-steel plates assembly and selected as master nodes to construct a kinematic coupling to the top/bottom surface of steel plates. In addition, for the columns that were confined by the FRCM-mortar assembly, an embedded region constraint was used to model the FRCM-to-mortar interaction. FRCM was positioned in the middle plane of the mortar section. Also, the mortar was bonded to the concrete, thus, the relative motion between the connected parts was 0, assuring full transfer of internal forces. Surface-to-surface interactions were defined between concrete/mortar parts and the steel plates, using the penalty contact method and finite sliding algorithm. A contact interaction property was used, having the tangential behavior of "Penalty" type with the friction coefficient set to 0.3 and the normal behavior set to "Hard" contact (no penetration). The reference points (RP1, RP2) were used to define the boundary conditions: a fixed support was assigned to one reference point (RP1) and a roller support was assigned to the other reference point (RP2). RP2 was used to apply the load as displacement control.

The FEM analyses were performed using the Dynamic Explicit solver and it consists of two

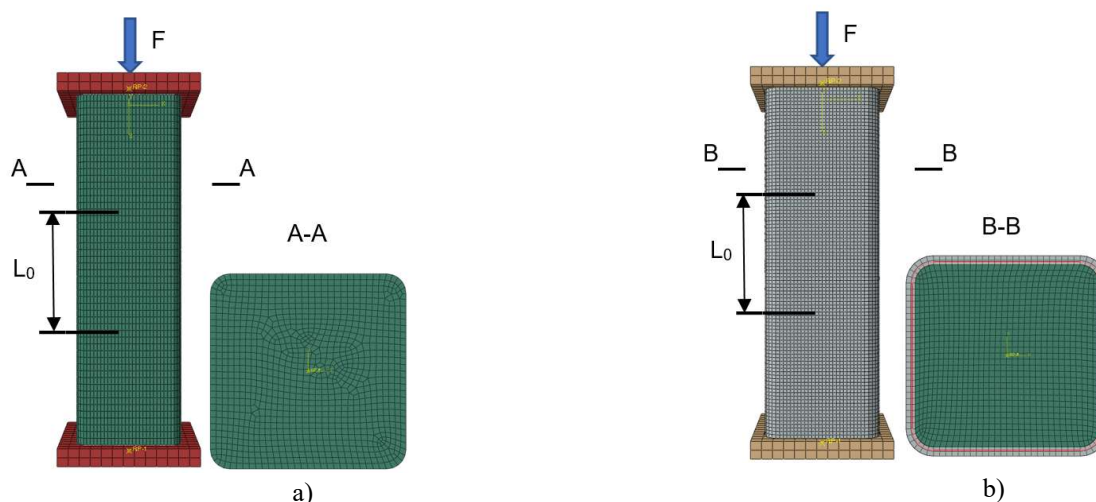


Fig. 3 - FEM models: a) CP-1 and CP-2, b) CP-3 to CP-6 / Modele FEM: a) CP-1 și CP-2, b) CP-3 până la CP-6.

steps. In the initial step the model is defined. In the second step, the load was applied using a smooth step amplitude to avoid dynamic effects and to assure a quasi-static analysis (displacement of 2.2 mm in a step time of 10 s). For the last step, nonlinear effects of large deformations and displacements were considered.

The output energies were checked to validate the numerical model: kinetic energy was under 1% of the internal energy, thus assuring a quasi-static analysis; artificial energy was also low, under 1% of the internal energy, thus validating the finite elements used (no shear locking of hourglass deformation modes of the elements). The output quantities of the simulations were the axial reaction force  $F$  from RP1, the relative displacement  $D$  of the reference points delimiting the gauge length, the stress and strain state.

### 3.3. Results

The predictions in terms of axial deformation – axial load curve are presented in Figure 2 in comparison with the experimental results. As a global overview, the FEM models reproduce the experimental response with a good level of accuracy; both the axial stiffness and the maximum axial load  $N_{max}$  are captured by the FEM models. The maximum axial load carrying capacity  $N_{max,FEM}$  was recorded and compared with the experimental results  $N_{max,exp}$ . Close predictions are obtained. The results are summarized in Table 5. The error was computed with the formula:  $error = ((N_{max,exp} - N_{max,FEM}) / N_{max,exp}) \cdot 100$ .

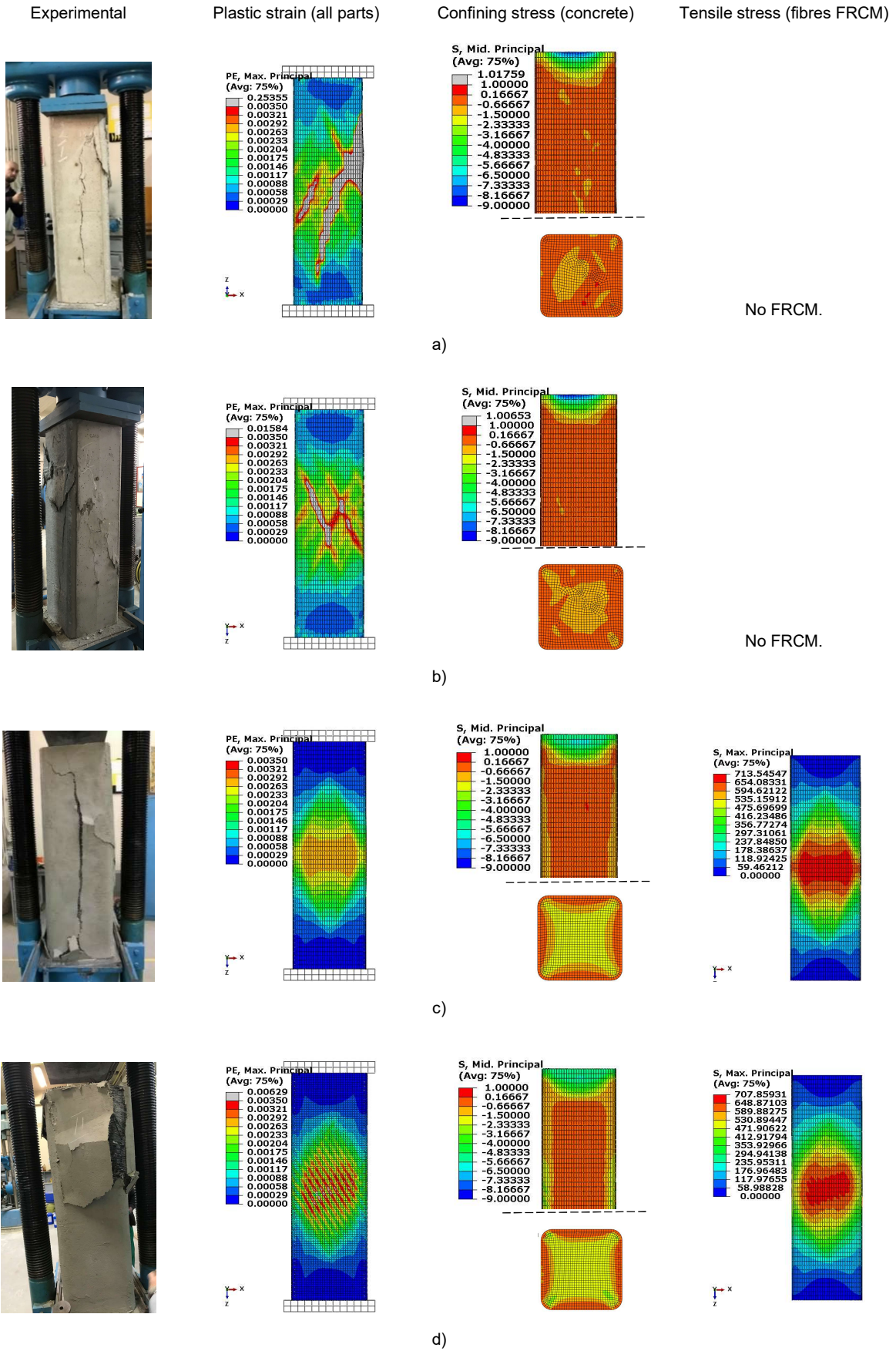
The failure of the column is a result of the cracks initiation and propagation throughout the element. The implementation of the concrete damaged plasticity model in Abaqus does not have the notion of cracks developing at the material integration point [14]. Instead, the concept of an effective crack direction was introduced with the purpose of obtaining a graphical visualization of the cracking patterns in the concrete structure.

Specimen	$N_{max,exp}$ [kN]	$N_{max,FEM}$ [kN]	Error [%]
CP-1	1830	1821	0.48%
CP-2	1920	1934	-0.71%
CP-3	2130	2038	4.30%
CP-4	2160	2159	0.05%
CP-5	2114	2006	5.10%
CP-6	2135	2129	0.28%

According to Lubliner et. al., as described in [14], crack initiation takes place at points where the tensile equivalent plastic strain ( $PEEQT$ ) is greater than zero,  $PEEQT > 0$ , and the maximum principal plastic strain is positive,  $PE.MAX.PRINCIPAL > 0$ . The direction of the vector normal to the crack plane is assumed to be parallel to the direction of the maximum principal plastic strain.

Figure 4 presents the failure modes numerically obtained in comparison with the experimentally recorded failure modes of all six columns. The values of the maximum principal plastic strains,  $PE.MAX.PRINCIPAL$ , are plotted at the end of analyses, which corresponds to the failure point. It can be observed that the crack patterns are similar to the experimental results.

For the evaluation of the variation of the concrete confining stresses the middle principal stress  $S.MID.PRINCIPAL$  was used as Abaqus output. Figure 4 presents the variation of  $S.MID.PRINCIPAL$  along the length of the column for concrete and mortar parts, and the variation of  $S.MID.PRINCIPAL$  in the section plane at the failure (last increment). Few general considerations are



a)

b)

c)

d)

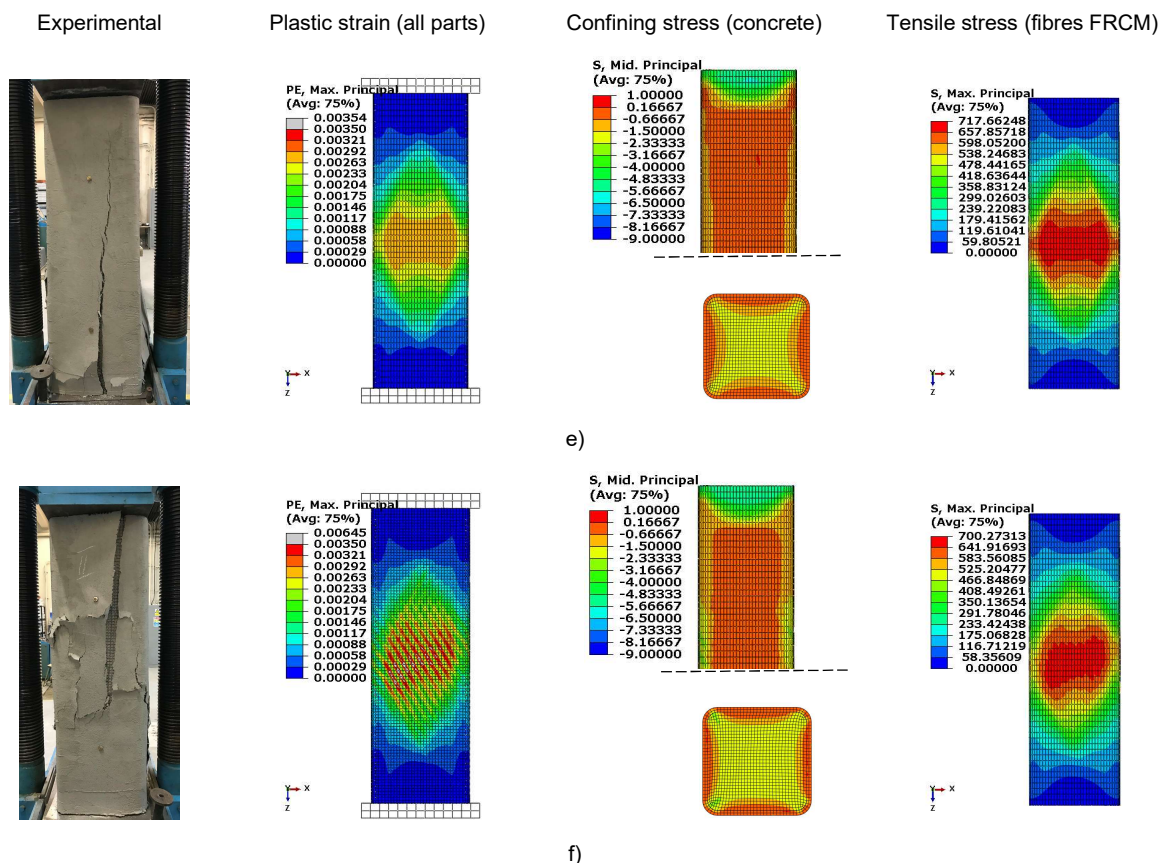


Fig. 4 – Experimental vs. FEM - failure mode, confining stresses in concrete part and tensile stresses in fibres (FRCM): a) CP- 1, b) CP- 2, c) CP-3, d) CP-4, e) CP-5, f) CP-6 / FEM vs. experimental - mod de cedare, eforturi de confinare in beton și eforturi de întindere in fibre (FRCM): a) CP-1, b) CP-2, c) CP-3, d) CP-4, e) CP-5, f) CP-6.

FEM results: principal strains and stresses / Rezultate FEM: deformații specifice și eforturi principale.			
Specimen	Concrete: PE.MAX.PRINCIPAL [mm/mm]	Concrete: +S.MID.PRINCIPAL [N/mm <sup>2</sup> ]	FRCM: S.MAX.PRINCIPAL [N/mm <sup>2</sup> ]
CP-1	0.25355	1.01759	-
CP-2	0.01584	1.00653	-
CP-3	0.00347	0.77391	714
CP-4	0.00336	0.85411	708
CP-5	0.00354	0.76790	718
CP-6	0.00335	0.88333	700

stated below. Negative values of *S.MID.PRINCIPAL* mean compression, while positive values mean tension. The level of confinement along the height of column is higher at the ends for both the concrete and the mortar part due to the presence of the friction forces at the contact with the steel plates. The distribution of the confining stresses and the level of confinement across the cross-section varies from unconfined models to the FRCM confined models. Better confinement is obtained for models with two layers of FRCM, compared to one-layer models. The results are summarized in Table 6 and only the maximum values (positive) of *S.MID.PRINCIPAL* were recorded since the minimum values are obtained in the contact area with the steel plates, and thus the cross-sectional

confinement is influence by the friction forces.

The tensile stress in the fibre jackets was evaluated using the maximum principal stress *S.MAX.PRINCIPAL*. Figure 4 presents the variation of *S.MAX.PRINCIPAL* along the length of the column for FRCM part, at the failure. The tensile stresses vary across the cross-section from the corners to center zones. Lower stresses are recorded at the corners. Slightly lower stresses are obtained for cases with two layers of FRCM (CP-4 and CP-6). For the models with one FRCM layer (CP-3 and CP-5), the tensile stresses are more concentrated in the mid height on column. The maximum values of *S.MAX.PRINCIPAL* recorded for each confined model are summarized in Table 6

#### 4. Analytical results

For design engineers, experimental and FEM evaluation techniques are not feasible for current design projects of retrofit. Therefore, simplified analytical formulations must be provided and used with a certain level of accuracy of prediction. Thus, in this section analytical predictions are presented in view of comparison with the experimental and the FEA results. In the study of Fosseti et al. [17] are presented a set of simplified analytical models for compressed concrete columns confined with FRCM system that were proposed over the years by various researchers [1, 3, 18-20]. All the analytical models are based on a general form described by equation (1), in which the confinement effect in terms of strength is expressed as function of the effective lateral confinement pressure  $f_{l,e}$ :

$$\frac{f_{cc}}{f_{co}} = \alpha + k_1 \left( \frac{f_{l,e}}{f_{co}} \right)^m \quad (1)$$

where:  $f_{co}$  : is the unconfined maximum compressive strength of specimens and is equal to initial compressive strength  $f_{c,initial}$  ;  $f_{cc}$  is the confined maximum compressive strength of specimens;  $\alpha$ ,  $k_1$  and  $m$  are non-dimensional

parameters experimentally evaluated. For FRCM jacketing, the factor  $k_1$  can be determined as  $k_1 = \alpha k_{1,R}$ , considering  $\alpha$  as an effectiveness coefficient which depend on the specifying jacketing system, and  $k_{1,R}$  as the non-dimensional parameter calibrated for specimens wrapped by FRCM system. For the evaluation of the effective lateral confinement pressure equation (2) is used:

$$f_{l,e} = \frac{1}{2} \rho_f E_f \varepsilon_f k_e \quad (2)$$

where  $\rho_f$  is the confinement ratio,  $E_f$  and  $\varepsilon_f$  are the elastic modulus and strain of the jackets in the lateral direction, respectively,  $k_e$  is the effectiveness coefficient that considers the variation of the confinement pressure in square and rectangular cross-section specimens with respect to circular ones, near corners.

The analytical predictions are summarized in Table 7. The best predictive results of increasing the axial strength were made by the model of Di Ludovico et al. [18]. The highest predictions for the increase in axial strength were obtained by model of Ombres [3]. The results for the axial compressive strength increase from Table 7 can be compared from de design point of view with the results from Table 2. The best results obtained with the model of

Analytical results of the confinement effect / Rezultate analitice ale efectului de confinare.					
Proposed model	Variables	Specimens			
		CP-3-	CP-5-	CP-4-	CP-6-
Triantafillou et al. [1] $\frac{f_{cc}}{f_{co}} = 1 + 1.9 \frac{f_{l,e}}{f_{co}}$	No. layers	1	1	2	2
	$f_{co} = f_{c,initial}$ (MPa)	19	18	19	18
	$f_{cc}$ (MPa)	20.67	19.67	22.34	21.34
	$f_{cc}/f_{co}$	1.09	1.09	1.18	1.19
	$f_{c,exp}$ (MPa)	23.67	23.49	24.00	23.72
	$f_{cc}/f_{c,exp}$	0.87	0.84	0.93	0.90
Di Ludovico et al. [18] $\frac{f_{cc}}{f_{co}} = 1 + 2.35x \left( \frac{f_{l,e}}{f_{co}} \right)^{0.85}$	No. layers	1	1	2	2
	$f_{co} = f_{c,initial}$ (MPa)	19	18	19	18
	$f_{cc}$ (MPa)	21.71	20.69	23.89	22.85
	$f_{cc}/f_{co}$	1.14	1.15	1.26	1.27
	$f_{c,exp}$ (MPa)	23.67	23.49	24.00	23.72
	$f_{cc}/f_{c,exp}$	0.92	0.88	1.00	0.96
De Caso Y Basalo et al. [19] $\frac{f_{cc}}{f_{co}} = 1 + 3.34 \frac{f_{l,e}}{f_{co}}$	No. layers	1	1	2	2
	$f_{co} = f_{c,initial}$ (MPa)	19	18	19	18
	$f_{cc}$ (MPa)	22.62	21.62	26.24	25.24
	$f_{cc}/f_{co}$	1.19	1.20	1.38	1.40
	$f_{c,exp}$ (MPa)	23.67	23.49	24.00	23.72
	$f_{cc}/f_{c,exp}$	0.96	0.92	1.09	1.06
Colajanni et al. [20] $\frac{f_{cc}}{f_{co}} = 2.254 \sqrt{1 + 7.94 \frac{f_{l,e}}{f_{co}}} - 2 \frac{f_{l,e}}{f_{co}} - 1.254$	No. layers	1	1	2	2
	$f_{co} = f_{c,initial}$ (MPa)	19	18	19	18
	$f_{cc}$ (MPa)	23.49	22.47	27.34	26.27
	$f_{cc}/f_{co}$	1.24	1.25	1.44	1.46
	$f_{c,exp}$ (MPa)	23.67	23.49	24.00	23.72
	$f_{cc}/f_{c,exp}$	0.99	0.96	1.14	1.11
Ombres [3] $\frac{f_{cc}}{f_{co}} = 1 + 5.268 \frac{f_{l,e}}{f_{co}}$	No. layers	1	1	2	2
	$f_{co} = f_{c,initial}$ (MPa)	19	18	19	18
	$f_{cc}$ (MPa)	26.42	25.42	33.85	32.85
	$f_{cc}/f_{co}$	1.39	1.41	1.78	1.83
	$f_{c,exp}$ (MPa)	23.67	23.49	24.00	23.72
	$f_{cc}/f_{c,exp}$	1.12	1.08	1.41	1.38

Di Ludovico et al. [18], the comparison yields close predictions for one layer of FRCM (the ration of  $f_{cc}/f_{c,exp}$  is 0.88~0.92) and for two layers of FRCM (the ration of  $f_{cc}/f_{c,exp}$  is 0.96~1.00)

## 5. Conclusions

In the first part of the paper the experimental results on six short low-strength plain concrete columns confined by FRCM are presented. Two columns, CP-3 and CP-5, were confined with one FRCM layer, two layers were used for CP-4 and CP-6, and no confinement for reference specimens CP-1 and CP-2. Adding one layer of FRCM provided the specimens CP-3 and CP-5 with an additional 13.17% capacity, relative to average capacity of reference specimens CP-1 and CP-2. A 14.53% capacity increase was obtained for two-layer specimens CP-4 and CP-6. The axial compressive strength obtained from the columns is compared with the initial compressive strength  $f_{c,initial}$  which is about 0.9 of the compressive strength of the cube. The increment in compressive strength was with an average ratio of 28% for one-layer specimens and 29% for two-layer specimens. Thus, there is a small difference in compressive strength between one- and two-layer specimens. FRCM system reduced the deformation of confined specimens, when compared to reference specimens. Two layers of FRCM (CP-4, CP-6) slightly reduced the deformation with respect to one-layer specimens (CP-3, CP-5). The failure mode of confined specimens was less brittle compared to unconfined specimens. The failure of confined specimens was observed at/near mid-height. The failure starts as a crack at mid-height of specimen and vertically grows to extremities of the specimen until the failure occurs.

A numerical FEM model was developed for each column and close predictions were obtained. Also, both the axial stiffness and the maximum axial load  $N_{max}$  are captured. The failure mode was assessed by evaluation of the maximum principal plastic strains; the crack patterns are similar to the experimental results. The confining stresses in the concrete was evaluated using the middle principal stress. It was concluded that: the level of confinement along the height of column is higher at the ends due to the presence of the friction forces at the contact with the steel plates; the distribution of the confining stresses and the level of confinement across the cross-section varies from unconfined to the confined models; better confinement is obtained for models with two layers of FRCM, compared to one-layer models.

Analytical models showed various values of predictions for the axial compressive strength increase. The best fit was obtained with the model proposed by Di Ludovico et al. [18]. To comparison

with test results, this comparison gives close predictions for one layer of FRCM (the ration of  $f_{cc}/f_{c,exp}$  is 0.88~0.92) and for two layers of FRCM (the ration of  $f_{cc}/f_{c,exp}$  is 0.96~1.00).

## REFERENCES

- [1] T.C. Triantafillou, C.G. Papanicolaou, P. Zissimopoulos and T. Laourdekis, Concrete confinement with textile-reinforced mortar jackets, *ACI Mater. J.*, 2006, **103**., 28.
- [2] A. Peled, Confinement of damaged and nondamaged structural concrete with FRP and TRC sleeves, *J. Compos. Constr.* 2007, **11**, 514-522.
- [3] L. Ombres, Concrete confinement with a cement based high strength composite material, *Compos. Struct.* 2014, **109**, 294-304.
- [4] T. Trapko, Effect of eccentric compression loading on the strains of FRCM confined concrete columns, *Constr Build Mater.* **61**, 97-105, 2014.
- [5] T. Trapko, Behaviour of fibre reinforced cementitious matrix strengthened concrete columns under eccentric compression loading, *Materials&Design* (1980-2015), 2014 **54**, 947-954.
- [6] L. Ombress. S. Verre, Structural behaviour of fabric reinforced cementitious matrix (FRCM) strengthened concrete columns under eccentric loading, *Comp.Part B.*, 2015, **75**, 235-249.
- [7] A. Jawdhari, A.H. Adheem, M.M. Kadhim, Parametric 3D finite element analysis of FRCM-confined RC columns under eccentric loading, *Eng. Struct.*; 2020, **212**, 1–14..
- [8] CEN - EUROPEAN COMMITTEE FOR STANDARDIZATION. Eurocode 2: Design of concrete structures – Part 1-1: General rules and rules for buildings, Eurocode 2-1-1/2004, 2004.
- [9] ASRO, SR EN 12390-3:2019 Testing hardened concrete. Compressive strength of test specimens, 2019.
- [10] Mapegrid C170, <https://www.mapei.com/it/en/products-and-solutions/products/detail/mapegrid-c-170>
- [11] Planitop HDM, <https://www.mapei.com/ro/ro/produse-si-solutii/lista-de-produse/detailu-referitor-la-produs/planitop-hdm>
- [12] F. Faleschini, M.A. Zanini, L. Hofer and C. Pellegrino, Experimental Behaviour of Reinforced Concrete Columns Confined with Carbon-FRCM Composites, *Construction and Building Materials*, 2020, **243**, 118296.
- [13] D. García, P. Alonso, J.T. San-José, L. Garmendia, C. Perlot, Confinement of medium strength concrete cylinders with basalt textile reinforced mortar, *Proc.13th Int.C.Pol.Concrete, ICPC, Portugal*, 2010.
- [14] ABAQUS, FEA. ABAQUS 6.14 Documentation. Dassault Systemes, Providence, RI, USA, 2014.
- [15] I. Cadar, T. Clipii, A. Tudor, *Beton armat*, ediția II-a, Ed. Orizonturi Universitare Timișoara, 2004.
- [16] N.F. Hany, E.G. Hantouche and M.H. Harajli, Finite element modeling of FRP-confined concrete using modified concrete damaged plasticity, *Engineering Structures*, 125, 1-14, 2016.
- [17] M. Fossetti, G. Alotta, F. Basone and G. Macaluso, Simplified analytical models for compressed concrete columns confined by FRP and FRCM system, *Materials and Structures*, 2017, **50**(6), 240.
- [18] M. Di Ludovico, A. Prota and G. Manfredi, Structural upgrade using basalt fibers for concrete confinement, *ASCE J Compos Constr* , 2010, **14**(5):541–552.
- [19] F.J. De Caso Y Basalo, F. Matta and A. Nanni, Fiber reinforced cement-based composite system for concrete confinement, *Constr Build Mater.* 2012 **32**, 55–65.
- [20] P. Colajanni, F. De Domenico, A. Recupero and A. Spinella, Concrete columns confined with fiber reinforced cementitious mortars: experimentation and modelling, *Constr Build Mater.* 2014, **52**, 375–384.

\*\*\*\*\*